

## Shock-induced band-gap shift in GaN: Anisotropy of the deformation potentials

H. Y. Peng, M. D. McCluskey,\* and Y. M. Gupta

*Institute for Shock Physics and Department of Physics, Washington State University, Pullman, Washington 99164-2816, USA*

M. Kneissl and N. M. Johnson

*PARC, Inc., 3333 Coyote Hill Rd., Palo Alto, California 94304, USA*

(Received 19 October 2004; published 24 March 2005)

The band-gap shift of GaN has been examined as a function of uniaxial compression along the  $c$  axis using time-resolved, optical absorption measurements in shock wave experiments. The hydrostatic deformation potential  $a_{cz}-D_1$  (parallel to the  $c$  axis), has been determined independently from  $a_{ct}-D_2$  (perpendicular to the  $c$  axis). Based on the experimental results, a set of deformation potentials has been obtained:  $a_{cz}-D_1=-9.6$  eV,  $a_{ct}-D_2=-8.2$  eV,  $D_3=1.9$  eV, and  $D_4=-1.0$  eV. These values indicate that the deformation potentials in wurtzite GaN are anisotropic.

DOI: 10.1103/PhysRevB.71.115207

PACS number(s): 71.55.Eq, 71.70.Fk, 62.50.+p, 78.40.-q

### I. INTRODUCTION

Wide band-gap III-nitride semiconductors have received considerable attention for their many applications in short-wavelength optical devices and high-power electronic devices. Despite the technological advances based on these materials, many of their fundamental physical properties have not been characterized.<sup>1</sup> In particular, the effect of strain on the optical properties is not well understood. Due to the large differences in lattice parameters and thermal expansion coefficients between the substrate (normally sapphire or SiC) and the different III-nitride epilayers, strain is always present in these devices. A more complete understanding of strain-induced effects on the band gap of GaN will improve the modeling of III-nitride optoelectronic devices.

For wurtzite GaN with small strains, four distinct valence-band and two conduction-band deformation potentials<sup>2,3</sup> are necessary to describe the band-edge variations. Three of these deformation potentials are used to characterize the effect of strain components along the  $c$  axis and the other three are used for strain components perpendicular to the  $c$  axis. The deformation potentials are derived from theoretical calculations,<sup>2-6</sup> where the parameters are fit to experimental data.<sup>7-12</sup> However, reported values are scattered over a large range, with variations of nearly a factor of 6 in some cases.

Commonly, quasicubic<sup>13</sup> or spherical cubic<sup>14</sup> approximations are introduced to reduce the number of unknown parameters. These approximations are based on the similarity between the wurtzite and zinc-blende crystal structures, which have nearly identical nearest-neighbor tetrahedral environments. For wurtzite GaN, deformation potentials have been obtained using hydrostatic pressure<sup>15-18</sup> and in-plane biaxial stress.<sup>7-12</sup> Since these methods involve strain components both along and perpendicular to the  $c$  axis, the cubic approximation is used to determine the deformation potentials. However, no experimental data are available to test the validity of such an approach.

In this paper, we present band-gap measurements for *uniaxial strain* along the  $c$  axis of wurtzite GaN. This unique method enables the direct measurement of the deformation potential along the  $c$  axis. Combining this result with other

published experimental data, we are able to determine the remaining deformation potentials. Our results suggest that the deformation potentials for wurtzite GaN are anisotropic and are not well described by the cubic approximation. Given the experimental data, the deformation potentials obtained in this work are expected to be more accurate than those published previously.

### II. EXPERIMENT

The samples used in this study were GaN:Mg and GaN:Si epilayers (4  $\mu\text{m}$  thick) on  $c$ -cut sapphire substrates (420  $\mu\text{m}$  thick) grown by metal-organic chemical vapor deposition. The band-gap shifts of these samples were studied as a function of uniaxial strain compression along the  $c$  axis using time-resolved, optical absorption measurements in shock-wave experiments. The experimental configuration is shown schematically in Fig. 1. Light from a xenon flashlamp was collimated and reflected by two turning mirrors mounted on the projectile and then passed through the impactor, GaN sample, and back window. The transmitted light was collected by an UV-transparent lens and focused onto two optical fibers. The light from one fiber was spectrally dispersed by a spectrometer (ARC SpectraPro 150), temporally dispersed by an electronic streak camera (Imacon 500), and digitally recorded on a charge-coupled device (CCD) detector as a series of transmission spectra, each separated in time by 20 ns. The second fiber delivered the transmitted signal to a fast photodiode, which was used as a timing diagnostic.  $C$ -cut sapphire single crystals were used for both the impactor and back window. Sapphire is transparent over a wide spectral range when shocked to stresses below the Hugoniot elastic limit (about 14 GPa).<sup>19</sup> From the measured projectile velocity, the stress in the GaN epilayer was determined by the shock response of a  $c$ -cut sapphire, which is known to an accuracy of 1%–2%.<sup>20</sup> A constant stress was maintained for 130 to 270 ns, depending on the size of each sample. All experimental data were collected within this time window.

Absorption spectra of GaN:Si shocked to 9.0 GPa are shown in Fig. 2. The absorption coefficient  $\alpha$  was obtained as a function of photon energy  $\hbar\omega$  using

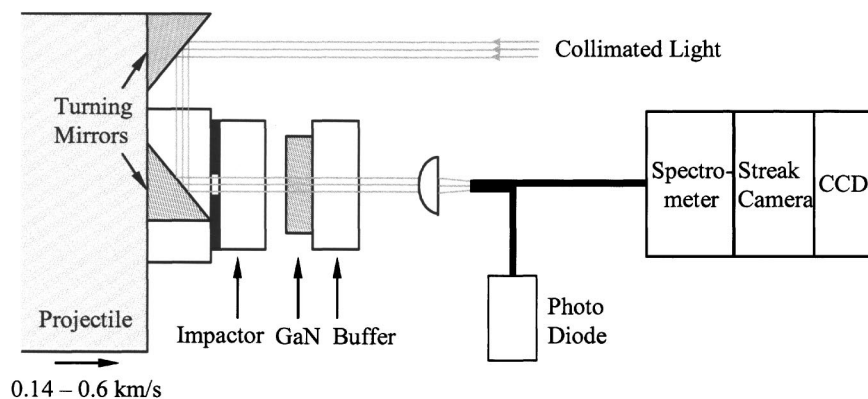


FIG. 1. Schematic diagram of the experimental configuration.

$$\alpha = \ln\left(\frac{I_0 - I_b}{I - I_b}\right) / d, \quad (1)$$

where  $I$  is the intensity transmitted through the sample (GaN+sapphire substrate),  $I_0$  is the intensity transmitted through the reference sample (sapphire substrate),  $I_b$  is the background intensity recorded with the streak camera shutter closed, and  $d$  is the thickness of the GaN epilayer. As can be seen from Fig. 2, the absorption spectrum shifted to higher energy upon arrival of the shock wave. The band-gap energy was defined to be the energy at which  $\alpha = 2.88 \times 10^3 \text{ cm}^{-1}$ . The band-gap shift  $\Delta E_g$  was taken to be the difference between the shocked band gap (120 ns after the initial shock) and the unshocked band gap.

The shift of the absorption edge measured at a constant value of  $\alpha$  will represent the band-gap shift only if the shape of the absorption profile does not change significantly.<sup>15</sup> However, GaN has large piezoelectric coefficients, and shock compression along its  $c$  axis will produce a large electric field along the same direction. This piezoelectric field results in a broadening of the absorption edge (Franz-Keldysh effect). In order to suppress the Franz-Keldysh effect, GaN:Mg (Ref. 21) and GaN:Si samples were used. The free carriers in these samples screen the piezoelectric field and thus reduce

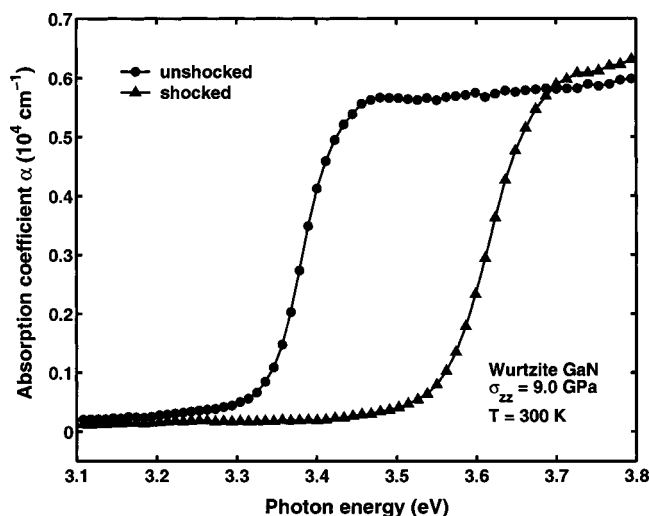


FIG. 2. Absorption spectra of GaN:Si before and after shock compression to 9.0 GPa.

the broadening of the band-gap threshold. For the determination of  $\Delta E_g$ , we only used the absorption spectra from GaN samples that showed *negligible broadening*<sup>22</sup> after shock compression. The plot of  $\Delta E_g$  as a function of longitudinal stress  $\sigma_{zz}$  is shown in Fig. 3.

### III. THEORY

#### A. Band gap

For wurtzite semiconductors,<sup>2,3</sup> the three valence bands HH ( $\Gamma_9^V$ ), LH ( $\Gamma_7^V$ ), and CH ( $\Gamma_7^V$ ) have energy maxima given by

$$E_0^{\text{HH}} = \Delta_1 + \Delta_2 + \lambda_e + \theta_e,$$

$$E_0^{\text{LH}} = (\Delta_1 - \Delta_2 + \theta_e)/2 + \lambda_e + \sqrt{[(\Delta_1 - \Delta_2 + \theta_e)/2]^2 + 2\Delta_3^2}, \quad (2)$$

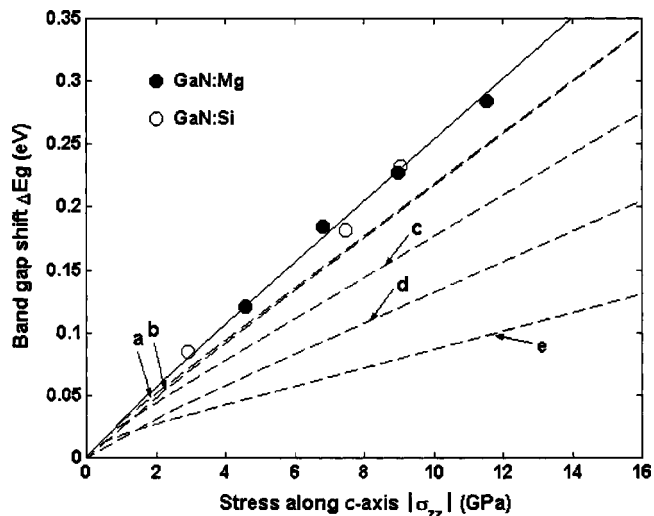


FIG. 3. The measured band-gap shift of GaN as a function of longitudinal shock stress  $\sigma_{zz}$ . The solid line is the best fit to the experimental data using deformation potentials obtained in this work, while the dotted lines are results expected by using values published in the literature: (a) Gil *et al.* (Ref. 7); (b) Tchoukeu *et al.* (Ref. 8); (c) Shan *et al.* (Ref. 12); (d) Chuang *et al.* (Ref. 2); (e) Kumagai *et al.* (Ref. 3). Here we use  $\Delta_1 = 8.4 \text{ meV}$  and  $\Delta_2 = \Delta_3 = 5.9 \text{ meV}$  (Ref. 25).

TABLE I. A comparison of linear slopes for  $A$ ,  $B$ , and  $C$  band-gap energies versus  $c$ -axis strain ( $\varepsilon_{zz}$ ) under biaxial stress ( $\perp$ ,  $c$  axis), hydrostatic pressure, and uniaxial strain ( $\parallel$ ,  $c$  axis) conditions.

| Band gap | Biaxial stress perpendicular to $c$ axis                           |   | Hydrostatic pressure  | Uniaxial strain along $c$ axis ( $\varepsilon_{zz} < 0$ ) |
|----------|--|---|---|---|
|          | $\varepsilon_{zz} < 0$   | $\varepsilon_{zz} > 0$  |   |   |
| $A$      | $(a_{cz} - D_1 - D_3) - \frac{C_{33}}{C_{13}}(a_{ct} - D_2 - D_4)$ | $(a_{cz} - D_1 - D_3) + \frac{2(C_{33} - C_{13})}{C_{11} + C_{12} - 2C_{13}}(a_{ct} - D_2 - D_4)$ | $(a_{cz} - D_1 - D_3) + \frac{2(C_{33} - C_{13})}{C_{11} + C_{12} - 2C_{13}}(a_{ct} - D_2 - D_4)$ | $(a_{cz} - D_1 - D_3)$                                    |
| $B$      | $(a_{cz} - D_1) - \frac{C_{33}}{C_{13}}(a_{ct} - D_2)$             | $(a_{cz} - D_1 - D_3) - \frac{C_{33}}{C_{13}}(a_{ct} - D_2 - D_4)$                                | $(a_{cz} - D_1) + \frac{2(C_{33} - C_{13})}{C_{11} + C_{12} - 2C_{13}}(a_{ct} - D_2)$             | $(a_{cz} - D_1)$  |
| $C$      | $(a_{cz} - D_1 - D_3) - \frac{C_{33}}{C_{13}}(a_{ct} - D_2 - D_4)$ | $(a_{cz} - D_1) - \frac{C_{33}}{C_{13}}(a_{ct} - D_2)$  | $(a_{cz} - D_1) + \frac{2(C_{33} - C_{13})}{C_{11} + C_{12} - 2C_{13}}(a_{ct} - D_2)$             | $(a_{cz} - D_1 - D_3)$                                    |

$$E_0^{\text{CH}} = (\Delta_1 - \Delta_2 + \theta_\varepsilon)/2 + \lambda_\varepsilon - \sqrt{[(\Delta_1 - \Delta_2 + \theta_\varepsilon)/2]^2 + 2\Delta_3^2},$$

where

$$\begin{aligned} \lambda_\varepsilon &= D_1 \varepsilon_{zz} + D_2 (\varepsilon_{xx} + \varepsilon_{yy}), \\ \theta_\varepsilon &= D_3 \varepsilon_{zz} + D_4 (\varepsilon_{xx} + \varepsilon_{yy}), \end{aligned} \quad (3)$$

where  $\Delta_1$  is the crystal-field splitting of the  $\Gamma_9$  and  $\Gamma_7$  orbital states,  $\Delta_2$  and  $\Delta_3$  are parameters that describe the spin-orbit coupling,  $\varepsilon_{ii}$  are components of the strain tensor, and  $D_i$  are valence-band deformation potentials. Here we use the convention that a positive (negative) value of  $\varepsilon_{ii}$  indicates tensile (compressive) strain. For the conduction band, the minimum energy is given by

$$E_0^{\text{C}} = \Delta_1 + \Delta_2 + E_g + a_{cz} \varepsilon_{zz} + a_{ct} (\varepsilon_{xx} + \varepsilon_{yy}), \quad (4)$$

where  $E_g$  is the band gap in the absence of strain and  $a_{cz}$  and  $a_{ct}$  are the conduction-band deformation potentials. Combining Eqs. (2)–(4) yields the band-gap shifts due to strain,

$$\begin{aligned} \Delta E_A &= (a_{cz} - D_1) \varepsilon_{zz} + (a_{ct} - D_2) (\varepsilon_{xx} + \varepsilon_{yy}) - D_3 \varepsilon_{zz} \\ &\quad - D_4 (\varepsilon_{xx} + \varepsilon_{yy}), \end{aligned} \quad (5)$$

$$\begin{aligned} \Delta E_B &= \frac{\Delta_1 + 3\Delta_2}{2} + \left( a_{cz} - D_1 - \frac{D_3}{2} \right) \varepsilon_{zz} + \left( a_{ct} - D_2 - \frac{D_4}{2} \right) (\varepsilon_{xx} \\ &\quad + \varepsilon_{yy}) - \sqrt{\left[ \frac{\Delta_1 - \Delta_2 + D_3 \varepsilon_{zz} + D_4 (\varepsilon_{xx} + \varepsilon_{yy})}{2} \right]^2 + 2\Delta_3^2}, \end{aligned}$$

$$\begin{aligned} \Delta E_C &= \frac{\Delta_1 + 3\Delta_2}{2} + \left( a_{cz} - D_1 - \frac{D_3}{2} \right) \varepsilon_{zz} + \left( a_{ct} - D_2 - \frac{D_4}{2} \right) (\varepsilon_{xx} \\ &\quad + \varepsilon_{yy}) + \sqrt{\left[ \frac{\Delta_1 - \Delta_2 + D_3 \varepsilon_{zz} + D_4 (\varepsilon_{xx} + \varepsilon_{yy})}{2} \right]^2 + 2\Delta_3^2}, \end{aligned}$$

where  $a_{cz} - D_1$  and  $a_{ct} - D_2$  are the “hydrostatic” deformation potentials parallel and perpendicular to the  $c$  axis, respectively.

### B. Strain relations

In the present study of shock compression along the  $c$  axis, the following *uniaxial strain* relations hold:

$$\varepsilon_{zz} = \sigma_{zz}/C_{33} \quad \text{and} \quad \varepsilon_{xx} = \varepsilon_{yy} = 0, \quad (6)$$

where  $C_{ij}$  are the elastic constants and  $\sigma_{ii}$  are components of the stress tensor. Wurtzite GaN thin films grown on sapphire

or SiC typically experience *biaxial stress* caused by the substrate:

$$\varepsilon_{zz} = -(2C_{13}/C_{33})\varepsilon_{xx} \quad \text{and} \quad \varepsilon_{xx} = \varepsilon_{yy} \neq 0. \quad (7)$$

Under *hydrostatic pressure*,  $\sigma_{zz} = \sigma_{xx} = \sigma_{yy}$ ; however, the compression is not isotropic,

$$\begin{aligned} \varepsilon_{zz} &= \frac{C_{11} + C_{12} - 2C_{13}}{C_{33}(C_{11} + C_{12}) - 2C_{13}^2} \sigma_{zz} \quad \text{and} \\ \varepsilon_{xx} = \varepsilon_{yy} &= \frac{C_{33} - C_{13}}{C_{33}(C_{11} + C_{12}) - 2C_{13}^2} \sigma_{zz}. \end{aligned} \quad (8)$$

In this work, we use the elastic constants given in Ref. 23:  $C_{11} = 390$  GPa,  $C_{12} = 145$  GPa,  $C_{13} = 106$  GPa, and  $C_{33} = 398$  GPa.

Using the strain relations given above, we calculated the slopes for the  $A$ ,  $B$ , and  $C$  band-gap shifts versus  $\varepsilon_{zz}$  (Table I). These linear shifts ignore the contribution from  $\Delta_3$  in Eq. (5), a good approximation for the range of strains in this study. If one neglects the strain-dependent variations of the exciton binding energies, which are small,<sup>3</sup> then the slopes shown in Table I also represent the shifts for  $A$ ,  $B$ , and  $C$  exciton resonance energies with respect to  $\varepsilon_{zz}$ . Since the absolute shifts of the conduction- and valence-band edges have not been measured independently, we will treat  $a_{cz} - D_1$  and  $a_{ct} - D_2$  as two independent deformation potentials. Since  $D_3$  was reported to be positive in all studies,<sup>2–12</sup> it is reasonable to assume that  $a_{cz} - D_1 - D_3$  is less than  $a_{cz} - D_1$ .

## IV. RESULTS

In this section, we use our shock compression results, along with previous studies involving hydrostatic pressure and biaxial stress, to calculate a set of deformation potentials.

### A. Shock compression

From Table I, it can be seen that under uniaxial shock compression ( $\varepsilon_{zz} < 0$ ), the lowest band-gap shift arises from the  $B$  band gap. Thus, the slope of the band-gap shift versus  $\varepsilon_{zz}$  is equal to  $a_{cz} - D_1$ . A least-square linear fit to the experimental data in Fig. 3 results in

$$\Delta E_B = (24.2 \text{ meV/GPa}) |\sigma_{zz}| = -9.6 \varepsilon_{zz} \text{ eV}. \quad (9)$$

Hence,  $a_{cz} - D_1 = -9.6$  eV. This value is compared to the previously reported deformation potentials in Table II. Our

TABLE II. Deformation potentials for wurtzite GaN in units of eV.

| $a_{cz}-D_1$   | $a_{ct}-D_2$   | $D_3$ | $D_4$ | Reference |
|----------------|----------------|-------|-------|-----------|
| -8.16          | -8.16          | 3.71  | 3.71  | a         |
| -8.16          | -8.16          | 1.44  | -0.72 | b         |
| -6.5           | -11.8          | 5.3   | -2.7  | c         |
| -4.78          | -6.18          | 1.4   | -0.7  | d         |
| -2.9           | -10.9          | 8.00  | -4.00 | e         |
| $a_{cz}+15.35$ | $a_{ct}+12.32$ | 3.03  | -1.52 | f         |
| $a_{cz}+13.87$ | $a_{ct}+13.74$ | 3.03  | -1.63 | g         |
|                |                | 5.73  | -2.86 | h         |
|                |                | 8.82  | -4.41 | i         |
| -9.6           | -8.2           | 1.9   | -1.0  | This work |

<sup>a</sup>Gil *et al.* (Ref. 7).

<sup>b</sup>Tchounkeu *et al.* (Ref. 8).

<sup>c</sup>Shan *et al.* (Ref. 12).

<sup>d</sup>Chuang *et al.* (Ref. 2).

<sup>e</sup>Kumagai *et al.* (Ref. 3).

<sup>f</sup>Suzuki *et al.* (Ref. 5).

<sup>g</sup>Suzuki *et al.* (Ref. 6).

<sup>h</sup>Chichibu *et al.* (Ref. 9).

<sup>i</sup>Shikanai *et al.* (Ref. 10) and Chichibu *et al.* (Ref. 11).

value for  $a_{cz}-D_1$  is larger in magnitude (more negative) than those found by most other groups.

### B. Hydrostatic pressure

Photoluminescence (PL) and reflectance studies of high-quality wurtzite GaN on sapphire under hydrostatic pressure revealed that the pressure coefficients for A, B, and C excitons are the same to within experimental uncertainty.<sup>24</sup> That observation places the following constraint on  $D_3$  and  $D_4$ :

$$D_3 + \frac{2(C_{33} - C_{13})}{C_{11} + C_{12} - 2C_{13}} D_4 = 0, \quad (10)$$

or  $D_3 = -1.8D_4$ . The linear pressure coefficient for free-standing GaN (Ref. 16) is

$$\Delta E = (41.4 \text{ meV/GPa}) |\sigma_{zz}| = -24.4 \epsilon_{zz} \text{ eV}, \quad (11)$$

where  $\sigma_{zz} = \sigma_{xx} = \sigma_{yy}$ . From Table I, we have the following relation:

$$(a_{cz} - D_1) + \frac{2(C_{33} - C_{13})}{C_{11} + C_{12} - 2C_{13}} (a_{ct} - D_2) = -24.4 \text{ eV}. \quad (12)$$

Using  $a_{cz}-D_1 = -9.6$  eV, we derive  $a_{ct}-D_2 = -8.2$  eV.

### C. Biaxial stress

To determine  $D_3$  and  $D_4$ , we need to consider the strain dependence of exciton resonance energies in GaN under biaxial stress. From Table I, the slope for C excitons ( $\epsilon_{zz} > 0$ ) is given by

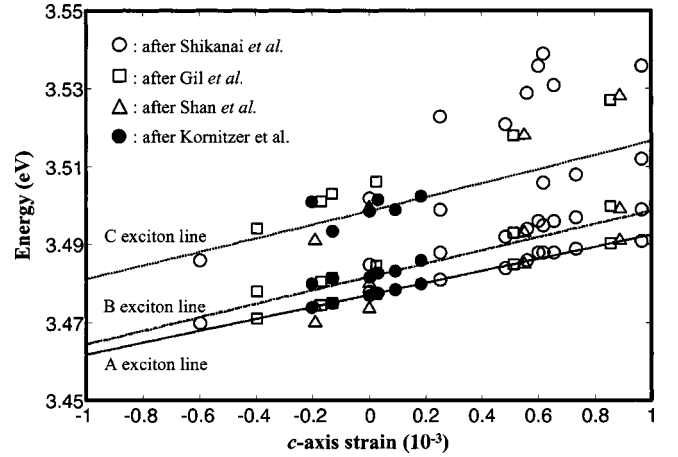


FIG. 4. A plot of the transition energies for A, B, and C excitons versus  $c$ -axis strain under biaxial stress. The symbols are experimental data presented by Shikanai *et al.* (Ref. 10), Gil *et al.* (Ref. 7), Shan *et al.* (Ref. 12), and Kornitzer *et al.* (Ref. 25), while the lines indicate calculation results predicted by this work. The slope of the A exciton line was taken to be 15.4 eV (Refs. 10 and 11) and the free exciton energies for strain-free GaN were taken from Ref. 25.

$$(a_{cz} - D_1) - \frac{C_{33}}{C_{13}} (a_{ct} - D_2) = 21.2 \text{ eV}. \quad (13)$$

This value is much smaller than the values of 38.9 and 34.5 eV, derived by Chichibu *et al.*<sup>10,11</sup> and Shan *et al.*,<sup>12</sup> respectively. The C exciton energies assigned by these authors are the highest-energy points in Fig. 4. However, our results suggest that these energies were misassigned. As pointed out by Kornitzer *et al.*,<sup>25</sup> misassignment of C exciton energies may occur easily for reflectance or PL studies made at very low temperatures.

From Table I, the difference between the slopes for A and C excitons with respect to  $\epsilon_{zz}$  is  $D_3 - (C_{33}/C_{13})D_4$ . Given a slope for  $E_A$  equal to 15.4 eV,<sup>10</sup> the slope difference is 5.8 eV. Using the fact that  $D_3 = -1.8D_4$ , we derive  $D_3 = 1.9$  eV and  $D_4 = -1.0$  eV. However, it should be noted that experimental uncertainties limit the accuracy of these values. We plotted the free exciton energies reported by different authors versus  $\epsilon_{zz}$  (symbols) under biaxial stress as well as the calculation results (lines) using these deformation potentials in Fig. 4. Our set of deformation potentials yield a good fit to the experimental data.

## V. DISCUSSION

In zinc-blende semiconductors, the hydrostatic deformation potentials  $a_c$  (conduction band),  $a_v$  (valence band), and the shear deformation potential  $b$  are used. For wurtzite semiconductors, the parameters  $D_1$  and  $D_2$  are analogous to  $a_v$ , while  $D_3$  and  $D_4$  are analogous to  $b$ . The hydrostatic deformation potentials shift the A, B, and C energy gaps uniformly, whereas the shear components lift the degeneracy of the valence bands at  $k=0$ . Our values for  $D_3$  and  $D_4$  are of the same magnitudes as the shear deformation potentials of zinc blende GaN [ $b = -1.6$  to  $-3.6$  eV (Ref. 26)] and other

*III-V* zinc-blende crystals<sup>27</sup> [e.g.,  $b = -1.7$  eV for GaAs (Ref. 28)]. Furthermore,  $D_3$  and  $D_4$  closely match the cubic approximation,  $D_3 = -2D_4$ .

However, the cubic approximation also states that  $(a_{cz} - D_1) - (a_{ct} - D_2) = D_3$ . Our results show that  $(a_{cz} - D_1) - (a_{ct} - D_2) = -1.4$  eV, which is different from  $D_3 = 1.9$  eV. Hence, the deformation potentials in wurtzite GaN show significant anisotropy. If we take into account the Franz-Keldysh effect, the band gap shift in Fig. 3 could be even higher, resulting in a larger magnitude for  $a_{cz} - D_1$  and a more pronounced anisotropy.

## VI. CONCLUSIONS

In summary, the band-gap shift of GaN under shock wave compression along its  $c$  axis has been measured using

time-resolved optical absorption experiments. The observed shift, 24.2 meV/GPa, is comparable to previous uniaxial-strain measurements that did not account for broadening.<sup>21,29</sup> The hydrostatic deformation potential along the  $c$  axis of wurtzite GaN,  $a_{cz} - D_1$ , has been determined experimentally to be  $-9.6$  eV. Combining this result with the known behavior of wurtzite GaN under hydrostatic pressure and biaxial stress, the deformation potentials have been estimated:  $a_{cz} - D_1 = -9.6$  eV,  $a_{ct} - D_2 = -8.2$  eV,  $D_3 = 1.9$  eV, and  $D_4 = -1.0$  eV.

## ACKNOWLEDGMENTS

H. Y. Peng thanks Kurt Zimmerman, Dan Dolan, and Gary Chantler for their help in performing the experiments. This research was supported by the U.S. Department of Energy, under Contract No. DE-FG03-97SF21388.

\*Electronic address: mattmcc@wsu.edu

<sup>1</sup>I. Vurgaftman, J. R. Meyer, and L. R. Ram-Mohan, *J. Appl. Phys.* **89**, 5815 (2001).

<sup>2</sup>S. L. Chuang and C. S. Chang, *Phys. Rev. B* **54**, 2491 (1996).

<sup>3</sup>M. Kumagai, S. L. Chuang, and H. Ando, *Phys. Rev. B* **57**, 15 303 (1998).

<sup>4</sup>T. Ohtoshi, A. Niwa, and T. Kuroda, *Jpn. J. Appl. Phys., Part 1* **35**, L1566 (1996).

<sup>5</sup>M. Suzuki and T. Uenoyama, *Jpn. J. Appl. Phys., Part 1* **35**, 1420 (1996).

<sup>6</sup>M. Suzuki and T. Uenoyama, *J. Appl. Phys.* **80**, 6868 (1996).

<sup>7</sup>B. Gil, O. Briot, and R. L. Aulombard, *Phys. Rev. B* **52**, R17 028 (1995).

<sup>8</sup>M. Tchounkeu, O. Briot, B. Gil, and J. P. Alexis, *J. Appl. Phys.* **80**, 5352 (1996).

<sup>9</sup>S. Chichibu, A. Shikanai, T. Azuhata, T. Sota *et al.*, *Appl. Phys. Lett.* **68**, 3766 (1996).

<sup>10</sup>A. Shikanai, T. Azuhata, T. Sota, S. Chichibu *et al.*, *J. Appl. Phys.* **81**, 417 (1997).

<sup>11</sup>S. Chichibu, T. Azuhata, T. Sota, H. Amano, and I. Akasaki, *Appl. Phys. Lett.* **70**, 2085 (1997).

<sup>12</sup>W. Shan, R. J. Hauenstein, A. J. Fischer, J. J. Song *et al.*, *Phys. Rev. B* **54**, 13 460 (1996).

<sup>13</sup>G. L. Bir and G. E. Pikus, *Symmetry and Strain-Induced Effects in Semiconductors* (Wiley, New York, 1974).

<sup>14</sup>Yu. M. Sirenko, J. B. Jeon, K. W. Kim, M. A. Littlejohn, and M. A. Stroschio, *Phys. Rev. B* **53**, 1997 (1996).

<sup>15</sup>D. L. Camphausen and G. A. N. Connell, *J. Appl. Phys.* **42**, 4438 (1971).

<sup>16</sup>P. Perlin, I. Gorczyca, N. E. Christensen, I. Grzegory *et al.*, *Phys. Rev. B* **45**, 13 307 (1992).

<sup>17</sup>W. Shan, T. J. Schmidt, R. J. Hauenstein, J. J. Song, and B. Goldenberg, *Appl. Phys. Lett.* **66**, 3492 (1995).

<sup>18</sup>P. Perlin, L. Mattos, N. A. Shapiro, J. Kruger *et al.*, *J. Appl. Phys.* **85**, 2385 (1999).

<sup>19</sup>R. L. Webb, M.S. dissertation, Washington State University, 1990.

<sup>20</sup>J. M. Winey and Y. M. Gupta, *J. Phys. Chem. A* **101**, 9333 (1997).

<sup>21</sup>H. Y. Peng, M. D. McCluskey, Y. M. Gupta, M. Kneissl, and N. M. Johnson, *Appl. Phys. Lett.* **82**, 2085 (2003).

<sup>22</sup>In Ref. 21, the slope of the absorption threshold was defined as  $d(\ln \alpha)/dE$ , where  $E$  is the photon energy. In the present study, we only included spectra that showed a slope decrease of  $\leq 30\%$  upon shock compression.

<sup>23</sup>A. Polian, M. Grimsditch, and I. Grzegory, *J. Appl. Phys.* **79**, 3343 (1996).

<sup>24</sup>Z. X. Liu, S. Pau, K. Syassen, J. Kuhl *et al.*, *Phys. Rev. B* **58**, 6696 (1998).

<sup>25</sup>K. Kornitzer, T. Ebner, K. Thonke, R. Sauer *et al.*, *Phys. Rev. B* **60**, 1471 (1999), and references therein.

<sup>26</sup>I. Vurgaftman, J. R. Meyer, and L. R. Ram-Mohan, *J. Appl. Phys.* **89**, 5815 (2001), and references therein.

<sup>27</sup>C. G. Van de Walle, *Phys. Rev. B* **39**, 1871 (1989).

<sup>28</sup>C. Y. P. Chao and S. L. Chuang, *Phys. Rev. B* **46**, 4110 (1992).

<sup>29</sup>M. D. McCluskey, Y. M. Gupta, C. G. Van de Walle, D. P. Bour, M. Kneissl, and N. M. Johnson, *Appl. Phys. Lett.* **80**, 1912 (2002).